

# Concept for Coring from a Low-mass Rover

Paul Backes\*, Oussama Khatib<sup>§</sup>, Antonio Diaz-Calderon\*, James Warren<sup>§</sup>, Curtis Collins\*, Zensheu Chang\*

\*Jet Propulsion Laboratory  
California Institute of Technology  
Paul.G.Backes@jpl.nasa.gov

<sup>§</sup>Department of Computer Science  
Stanford University  
ok@robotics.stanford.edu

*Abstract*— Future Mars missions, such as the Mars Sample Return (MSR) mission, may benefit from core sample acquisition from a low-mass rover where the rover cannot be assumed to be stationary during a coring operation. Manipulation from Mars rovers is currently done under the assumption that the rover acts as a stationary, stable platform for the arm. An MSR mission scenario with a low-mass rover has been developed and the technology needs have been investigated. Models for alternative types of coring tools and tool-environment interaction have been developed and input along with wheel-soil interaction models into the Stanford Simulation & Active Interfaces (SAI) simulation environment to enable simulation of coring operations from a rover. Coring tests using commercial coring tools indicate that the quality of the core is a critical criterion in the system design. Current results of the models, simulation, and coring tests are provided.

## TABLE OF CONTENTS

1. INTRODUCTION.....	1
2. ROVER-TOOL CONCEPT .....	1
3. CORING TOOL MODELS .....	2
4. SIMULATION ENVIRONMENT .....	5
5. WHEEL-SOIL INTERACTION .....	7
6. CORING TESTBED.....	8
7. RESULTS .....	8
8. CONCLUSIONS .....	9
ACKNOWLEDGEMENTS .....	9
REFERENCES .....	9
BIOGRAPHY .....	10

## 1. INTRODUCTION

Core sample acquisition from a planetary rover currently requires that the rover be a stationary platform for a manipulation system on which a coring tool is mounted. Future Mars rover missions, such as a Mars Sample Return (MSR) mission, may need to minimize mission cost by reducing the rover mass. With a low-mass rover, the interaction forces between the tool and terrain may cause the rover to slip during a coring operation. A research activity is underway to investigate how to enable coring from a low-mass rover. A rover-tool concept has been developed to act as the context for the work. Alternative core sampling tool concepts are being investigated and

modeled to determine what type of tool would be preferable for the low-mass rover system. A simulation system has been developed for simulating coring operations. A coring testbed has been developed to test core sample acquisition.

## 2. ROVER-TOOL CONCEPT

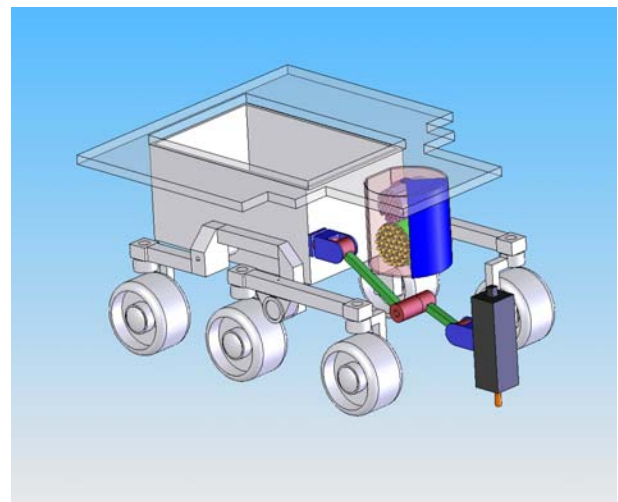
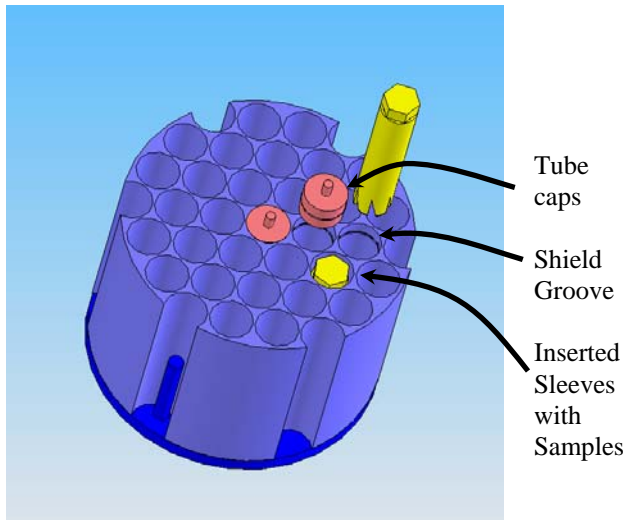


Figure 1. Rover-tool concept

The baseline operations scenario is to be able to acquire cores with the rover on slopes up to 30° with the tool at various angles relative to the rover. A vertical orientation of the tool will cause the lowest slip force while a horizontal orientation provides the highest slip force opposing the wheel traction.

A baseline rover-tool concept was developed to enable core sample acquisition for an MSR-type mission. The rover-tool system is shown in Figure 0. A first step was to decide how many degrees of freedom (DOFs) to have in the manipulation system that holds the coring tool. The earlier Athena rover concept for sample acquisition used a two DOF pitch-translate mechanism [1]. This activity chose a five DOF arm because it allows arm motion to accommodate rover slip in any direction. A two DOF arm requires that the rover act as a stationary platform or provide a mobility DOF during compensation for slip. But it is expected that the resolution of motion available from



**Figure 2. Sample container**

rover mobility will be too coarse to compensate for rover slip during coring.

Use of a three DOF arm, implemented by freezing two DOFs of the five DOF arm, will be investigated. If it is assumed that slippage will occur along the gravity vector projected onto a ground plane, then accommodation in a plane is all that will be required. Means for accommodating slippage in other directions will need to be included also.

Another consideration for the arm DOF is transfer of a sample to the sample container. A five DOF arm reduces the constraints on mounting of the sample container.

Sample contamination is a significant concern for a sample return mission. One approach for minimizing sample contamination is to acquire the sample directly into a storage sleeve. A sampling and containerization approach using a sample sleeve was developed, as shown in Figure 0. Bits with internal sleeves are stored in a bit station. One bit is used per core sample. Coring holes are started by percussion-only mode with the coring tool and then rotary percussion is used to acquire the core. The core is broken by rotating off-axis concentric tubes or by rotating cutting fingers at the end of the sleeve. Fingers at the end of the sleeve contain the sample in the sleeve and the sleeve is extracted from the bit. A tube cap is removed from the sample container using another tool on the arm turret and then the sleeve is inserted in the tube and seated in the shield groove.

### 3. CORING TOOL MODELS

The type of coring tool used to acquire the sample is very important. Different types of coring tools require different control relative to their environment and produce different quality cores. There are three basic types of coring tools for Mars sampling missions: rotary friction, ultrasonic, and rotary hammer.

#### *Rotary-Friction Coring Tool Model*

Rotary friction coring tools impart normal and tangential forces into the material. Large normal forces cause the bit teeth to catch and compress the rock surface and the rotary action causes tension or shear stress buildup that is relieved by the formation of tension or shear fractures along the direction of tooth motion [2]. There are two primary drawbacks of rotary friction coring tools, the relatively large normal force, or preload, required between the bit and rock and the need for a centering bit to start a coring hole. For coring from a low-mass rover, the large normal force required affects the rover mass by requiring the tool deployment device to apply this force against the environment. An example of this type of coring tool is the Mini-corer from Honeybee Robotics [3].

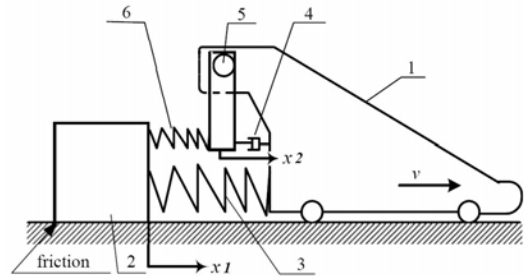


**Figure 3. The planar model of the rotary-friction drill system. 1: Drive with constant velocity  $v$ ; 2: tip of the bit with mass  $m_1$ ; 3: main spring with stiffness  $k_1$ ; 4: dashpot with viscous coefficient  $c_2$ ; 5: pin, attached with a lever with mass  $m_2$ ; 6: secondary spring with stiffness  $k_2$ .**

A model for rotary friction coring tools was proposed by Batako [5] to simulate the motion of a rotary corer with and without percussive actions. The model focuses on the tip of the corer bit. The movement of the tip of the corer bit is modeled as a stick-slip motion. The tip of the bit is connected to the shaft of the motor through the corer stem which is represented by a spring-damper system, as shown in the planar model in Figure 0. Note that the velocity  $v$  is the linear speed of the bit rotation; the lever connected to the drive at pin 5 is free to rotate; and there is dry friction between the bit and the surface of rock. The shaft of the motor is assumed to be rotating at a constant velocity. A

preload is applied to the corer system, and the corer bit is pressed against the rock. When the motor just starts working, the tip of the bit sticks to the rock due to friction; and then when the maximum static friction is reached, the tip of the bit slips until it sticks again. The stick-slip cycle repeats itself and such motion is known as “stick-slip motion”.

The governing equations of the motion of the tip of the corer bit are:

$$m_1 \ddot{x}_1 = -k_1 x_1 - k_2 (x_1 - x_2) - F_r(\dot{x}) \quad (1)$$

$$m_2 \ddot{x}_2 = -c_2 \dot{x}_2 - k_2 (x_2 - x_1)$$

where  $F_r(\dot{x})$  is the friction force,

$$F_r(\dot{x}) = \begin{cases} f_{st} \left( 1 - \frac{|\dot{x}|}{v_{cr}} + \frac{|\dot{x}|^3}{3v_{cr}^3} \right) \text{sgn}(\dot{x}) & \text{for } \dot{x} \neq 0 \\ \min[k_1 x_1 + k_2 (x_1 - x_2), f_{st}] \text{sgn}(k_1 x_1 + k_2 (x_1 - x_2)) & \text{for } \dot{x} = 0 \end{cases} \quad (2)$$

where  $f_{st}$  is the maximum static friction, and  $x = x_l + vt$ ;  $x_l$  and  $x_2$  are the coordinates of the bit and the lever, respectively, relative to drive 1.

A computer program was developed in Matlab/Simulink to solve the governing equations. To verify the validity of the computer program, the example problem shown in the paper [5] was solved by the program. It is found that the computer program we developed successfully repeated the results shown in the paper. We then modified the variables,  $m_1$ ,  $m_2$ ,  $k_1$ ,  $k_2$ ,  $c_2$ , and  $v$ , in the program to simulate the rotary-friction corer under investigation, the Mini-Corer developed by Honeybee. Some of the parameters in the model are not available, for example, the spring constants, equivalent mass of the bit-head (not the whole bit), etc. So we chose some values for these parameters so the results are compatible with the data we received from Honeybee including the rotational speed (about 200 RPM), the preload (155 N), and the average torque (2 N-m), etc. The preload (155 N) is also felt by the robotic arm, and it is taken as a constant in the model.

The model depicted in Figure 0 gives us the friction force between the drill bit and the surface of the rock, as well as the torque that exists in the drill stem. However, what we need is the torque felt by the robotic arm that holds the drill. So we modified the model to predict also the rotational speed of the rotor of the motor which drives the drill stem, and through the torque-rotational speed relationship we are

able to derive the torque that was delivered from the stator to the rotor. The torque delivered across the stator-rotor interface is actually the torque that the robotic arm needs to provide to hold the drill.

Figure 0 shows the dynamic torque that transmitted from the corer to the robotic arm. It is predicted by the model that the torque reaches the steady state after a short period of transient state. It should be noted that the solution is not unique, since there are more than one combination of variables in the model which would satisfy the specifications of the corer. To be able to predict the reaction forces more precisely, we need to know the spring constants,  $k_1$  and  $k_2$ , the mass,  $m_1$  and  $m_2$ , and the damping coefficient  $c_2$ , that characterize the corer bit.

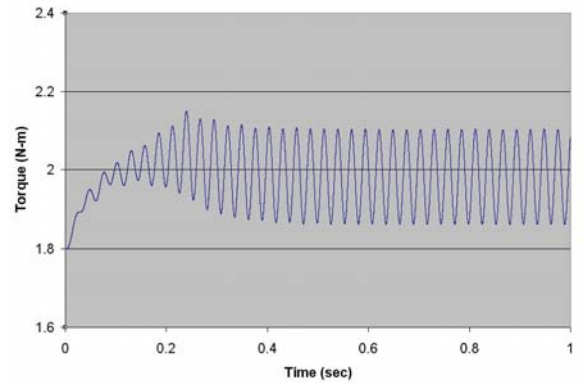


**Figure 4. Torque produced by a rotary friction coring tool**

#### *Rotary-Percussive Coring Tool Model*

The model of a self-excited rotary-percussive corer proposed by Batako [5] is shown in Figure 0. The impact loading is provided by the striker with mass  $m_2$ . At impact the friction force increases sharply, and it confines the bit to decelerate and to come to rest. The parameters of the system strongly affect each other, therefore a proper correlation of masses and stiffness in the system is needed for the process to converge to a stable solution.

The governing equations, from Batako, of the motion are:

$$\begin{aligned} m_1 \ddot{x}_1 &= -k_1 x_1 - k_2 (x_1 - x_2) - F_r(\dot{x}) + \Phi(x_2, \dot{x}_2) \\ m_2 \ddot{x}_2 &= -c_2 \dot{x}_2 - k_2 (x_2 - x_1) - \Gamma(x_2, \dot{x}_2) \end{aligned} \quad (3)$$

where  $F_r(\dot{x})$  is the friction force,

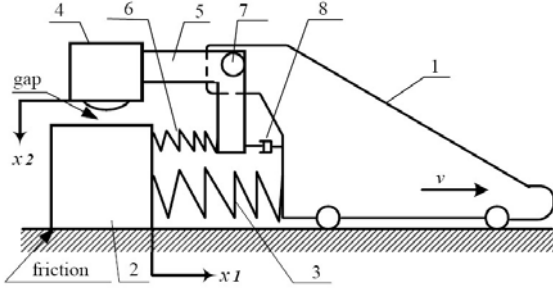


**Figure 5. The planar model of the rotary-percussive drill system. 1: Drive with constant velocity  $v$ ; 2: tip of the bit with mass  $m_1$ ; 3: main spring with stiffness  $k_1$ ; 4: striker with mass  $m_2$ ; 5: lever; 6: secondary spring with stiffness  $k_2$ ; 7: pin; 8: dashpot with viscous coefficient  $c_2$ .**

$$F_r(\dot{x}) = \begin{cases} f_{st} \left( 1 - \frac{|\dot{x}|}{v_{cr}} + \frac{|\dot{x}|^3}{3v_{cr}^3} \right) \text{sgn}(\dot{x}) & \text{for } \dot{x} \neq 0 \\ \min[f_{st}, k_1 x_1 + k_2(x_1 - x_2)] \text{sgn}(k_1 x_1 + k_2(x_1 - x_2)) & \text{for } \dot{x} = 0 \end{cases} \quad (4)$$

and  $f_{st} = \mu m_1 g$  is the static friction force, and  $\mu$  is the coefficient of static friction.

$\Gamma(x_2, \dot{x}_2)$  is the impact force which is defined as follows:

$$\Gamma(x_2, \dot{x}_2) = \begin{cases} k_0(x_2 - \Delta) + c_0 \dot{x}_2 & \text{for } x_2 \geq \Delta \text{ and } \Gamma(x_2, \dot{x}_2) > 0 \\ 0 & \text{for } x_2 \geq \Delta \text{ and } \Gamma(x_2, \dot{x}_2) < 0 \\ 0 & \text{for } x_2 < \Delta \end{cases} \quad (5)$$

where  $k_0$  is constant stiffness of the bit and  $c_0$  is constant damping, and  $\Delta$  is the initial gap between bit and striker.

$\Phi(x_2, \dot{x}_2)$  is the added friction force due to impact:

$$\Phi(x_2, \dot{x}_2) = \mu \Gamma(x_2, \dot{x}_2) \quad (6)$$

Since the rotary-percussive corer we want to model is actually a “forced” impact system instead of a self-excited one, we have modified the model shown in Figure 0 accordingly. The impact is created mechanically by a cam-spring system. The cam is fixed onto the drill stem, and while the stem rotates, the cam strains the spring and releases it periodically to create the impact. It is assumed that the cam-spring system creates three impacts with each rotation of the drill stem, and since the rotation speed of the stem is about 800 RPM, the impact rate is about 40 impacts per second. Equation (5), the impact force is rewritten as,

$$\Gamma(t) = \begin{cases} a_0 \sin(2\pi f t) & \text{for } 0 < t < 0.0001, 0.025 < t < 0.0251, \\ & 0.05 < t < 0.0501, \dots \\ 0 & \text{otherwise} \end{cases} \quad (7)$$

where the impact force is assumed to be sinusoidal with a frequency  $f$ , and  $f$  is assumed to be 5000 Hz. So the duration of the impact is 1000 micro-seconds. The  $a_0$  is the amplitude of the impact, and it is assumed to be 200 N. And Equation (6), the added friction force, is rewritten as,

$$\Phi(t) = \mu \Gamma(t) \quad (8)$$

Upon careful inspection of the Equation (3), it is found inadequate to add the “added friction force” directly to the governing equation. Instead, it should be treated as an increase of normal force between the drill bit and the surface of the rock, and be added to the static friction force,  $f_{st}$ , as shown in Equation (4). So both Equations (3) and (4) are rewritten as,

$$\begin{aligned} m_1 \ddot{x}_1 &= -k_1 x_1 - k_2(x_1 - x_2) - F_r(\dot{x}) \\ m_2 \ddot{x}_2 &= -c_2 \dot{x}_2 - k_2(x_2 - x_1) - \Gamma(x_2, \dot{x}_2) \end{aligned} \quad (9)$$

and

$$F_r(\dot{x}) = \begin{cases} (f_{st} + \Phi(t)) \left( 1 - \frac{|\dot{x}|}{v_{cr}} + \frac{|\dot{x}|^3}{3v_{cr}^3} \right) \text{sgn}(\dot{x}) & \text{for } \dot{x} \neq 0 \\ \min[f_{st} + \Phi(t), k_1 x_1 + k_2(x_1 - x_2)] \text{sgn}(k_1 x_1 + k_2(x_1 - x_2)) & \text{for } \dot{x} = 0 \end{cases} \quad (10)$$

Figure 0 shows the time history of the torque generated by a rotary-percussive corer with 155 N preload, and transmitted to the robotic arm which holds the corer. All the conditions

and parameters used in this model are the same as the ones used for the rotary-friction model, except that periodical impact is imposed upon the drill bit here. Compared with the torque created by a rotary-friction corer, shown in Figure 0, the average torque shown in Figure 0 is higher. Also, the peaks of the torque in Figure 0 oscillate due to the periodical impact.

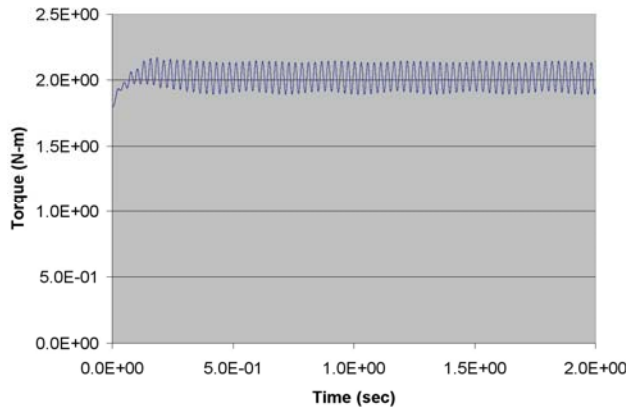


**Figure 6. Torque generated by a rotary-percussive coring tool with 155N preload**

Figure 0 shows the time history of the torque generated by a rotary-percussive corer with 50 N preload. Compare to Figure 0 where the preload is 155 N, the average torque here is lower. The phenomenon is expected since lower preload creates lower friction which results in lower torque. Additionally, when the preload is higher, the dynamic torque reaches its steady state faster.

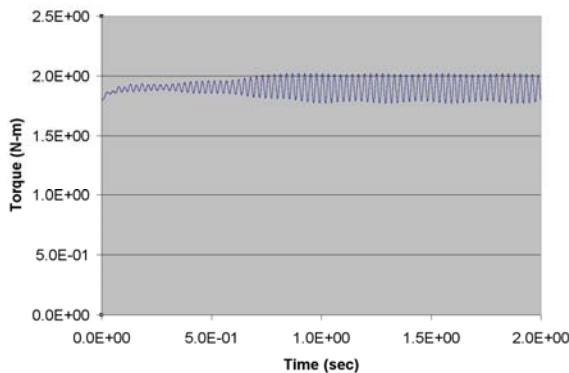


**Figure 7. Torque generated by a rotary-percussive coring tool with 50N preload**

### Ultrasonic Coring Tool Model

An ultrasonic drill/coring tool (USDC) consists of three main parts: an ultrasonic transducer (piezoelectric stack, a backing element, and a horn), free-mass and a drill stem. The ultrasonic transducer vibrates at a frequency of about 20 kHz. These vibrations of the horn tip excite the free-mass, causing it to hop between the horn tip and the top of the drill stem at frequencies around 1000 Hz. The free-mass transfers energy from the ultrasonic transducer to the drill stem. In order to determine the reaction force transmitted from the USDC to the robotic arm, a computer program was developed to simulate the interaction between the ultrasonic horn and the free mass, and between the free mass and the drill bit [4]. Time history of the location of the ultrasonic horn was predicted by the program, and it is assumed that the ultrasonic horn is connected to the robotic arm through a spring. Thus the reaction force can be calculated with the location of the ultrasonic horn and the spring constant available. Specifications for a USDC prototype are shown in Table 0. Figure 0 shows the time history of the reaction force.

**Table 1. Specifications of Prototype USDC**

Mass	0.3 kg
Envelope	4 cm dia. × 25 cm
Power	40 watt
Resonance Frequency	22500 Hz
Free mass	2 g

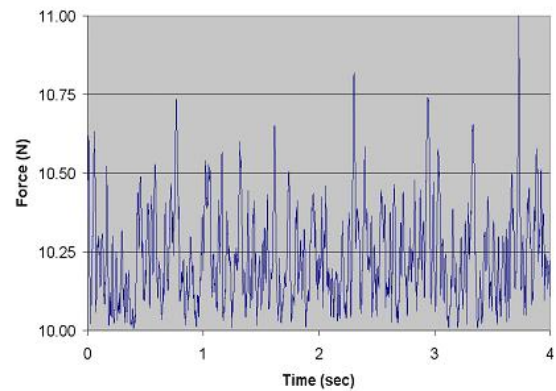


**Figure 8. USDC Reaction Force**

## 4. SIMULATION ENVIRONMENT

The cost of experimentation for rover design and control can be significantly reduced by developing a high fidelity virtual environment. Collaboration with Stanford University has led to the development of SAI [8] (Simulation & Active Interfaces), a simulation tool to assist

with the redesign, reconfiguration and control of low-mass rovers. SAI is unique in that it is a real-time interactive environment that allows the user to apply and sense forces within the virtual world via haptic devices. For the purposes of rover simulations, SAI features multi-contact resolution for multi-body systems, efficient algorithms for articulated body dynamics, and simulated friction and ground reaction forces.

SAI is based upon a general framework [7] for the resolution of multi-contact between articulated multi-body systems in the context of operational space control for robots [9]. Using this framework, the dynamic relationships between all existing contact points can be described. These relationships are characterized by the masses as perceived at the contact points. A force exerted at a contact point, whether from a collision with another object or from interaction with a user, can be translated into forces at all related contact points. The necessary computations can be performed with an efficient recursive algorithm.

The contact space representation allows interaction between groups of dynamic systems to be described easily without having to examine the complex equations of motion of each individual system. A collision model can be developed with the same ease as if one were considering interaction only between simple bodies. Impact and contact forces between interacting bodies can then be solved efficiently.

The simulation of articulated body dynamics moving in free space has led to a recursive algorithm for computing the operational space dynamics and control of an  $n$ -joint branching, redundant, articulated robotic mechanism with  $m$  operational points [6]. An operational point is a point on the robot at which a certain behavior is controlled; in most cases it represents an end effector. The computational complexity of this algorithm is  $O(nm + m^3)$ ; existing symbolic methods require a computational effort of  $O(n^3 + m^3)$ . Since  $m$  can be considered as a small constant in practice, the algorithm attains a linear time  $O(n)$  as the number of links increases. SAI integrates this framework with a haptic rendering system to provide a general environment for interactive haptic dynamic simulation.

Since SAI was initially designed as a robotic research tool, certain modifications were made to customize the software for rover simulations. Most of these changes were required to refine the interaction between the wheels and the surrounding terrain. The translational motion of wheeled robots was previously represented by two planar prismatic joints; now the translational effect of the rotation of each wheel is individually modeled. This change in the modeling of translational motion necessitated refinements in the friction models between the wheels and the soil. Grip and dynamic friction were added to static and viscous friction models to provide a means of representing different soil types the rover will encounter on Mars. Furthermore, since SAI currently models all objects as rigid bodies, the effect

of wheel sinkage was approximated by artificially increasing the contact area of the wheel in proportion to the expected sinkage depth.



**Figure 9. SAI simulation of the Rocky8 rover performing a coring task. The ground reaction forces are denoted by blue vectors whose length is proportional to the force magnitude.**

One of the major applications of SAI is to simulate the extraction of core samples from the surface of Mars. With the aforementioned modifications, SAI is well suited to test different rover designs and develop appropriate control strategies for this task. The user may analyze different design options in a multitude of coring scenarios (different terrain slopes and friction profiles). Moreover, different coring tools may be evaluated in SAI by specifying the expected forces and moments applied by the tool (Figure 0). Using SAI to resolve the resulting ground reaction forces allows the user to determine the effects of using a certain tool for a specific task. The ability to analyze these options in simulation will reduce the time and cost for rover development.

To increase the likelihood of success, the rover should remain stationary while extracting cores. The capability of SAI to efficiently determine ground reaction forces and simulate friction forces provides the ability to determine the region of coring tool contact forces that can be applied without causing slippage at the wheels. This analysis can assist in evaluating different coring tools as well as determine the minimum required mass of a rover to successfully core using a given tool.

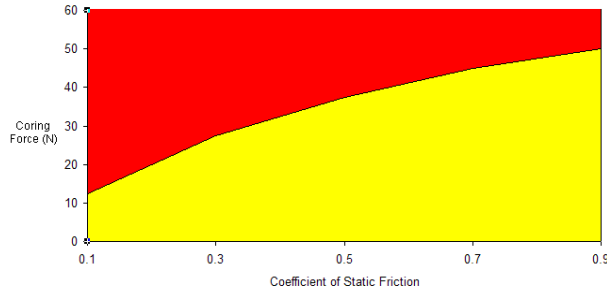


**Figure 10. Simulated wheel slippage force boundary determined via SAI simulations. Yellow region denotes stable forces, red region predicts wheel slippage.**

The scenario for this discussion involves the Rocky8 rover on flat terrain. A 5 DOF arm is mounted at the front left of the rover and is fully extended in the horizontal direction. The coring tool is percussive (zero contact moment) and applies a horizontal coring force. There is no assumed wheel sinkage, and gravitational forces consistent with Mars gravity are applied to the rover. During the simulations, the actuated joints are controlled to maintain the given configuration. The applied coring force is incrementally increased until movement is observed at the rover wheels. By repeating this simulation for different friction profiles, the slippage boundary depicted in Figure 0 is determined. It should be noted that the computed slippage boundary is an approximation, but accuracy will be significantly improved with the use of more representative terrain models

Similar to the previous example, SAI will be used as an evaluative tool for many other design decisions. By determining the optimal choices of coring tool type, 4 or 6 wheel base, arm mounting location and other design criteria, SAI addresses the overall goal of minimizing the required mass required to successfully perform coring tasks. SAI can also be used to evaluate different control strategies. In particular, SAI can help determine the optimal rover placement, wheel and arm configuration, and coring direction to increase the likelihood for successful core extraction. Moreover, should wheel slippage be detected, SAI can assist in designing control strategies to use the rover degrees of freedom to assist in stabilizing the rover.

## 5. WHEEL-SOIL INTERACTION

A wheel-soil interaction model was developed to estimate the traction available at the rover wheels to react coring operation forces. The baseline design consists of a 62 kg 6 wheel rocker-bogie rover (Rocky 8), a 5 DOF arm, and a conceptual coring tool. During the coring operation, the coring tool requires forces and torques to be applied along and about the coring tool axis. These forces will be

transmitted to the rover and to the ground through wheel/soil interaction. If the coring forces exceed the traction forces, the rover will slip.

Three elements are required to predict the available traction force. The first is a wheel/soil interaction model, the second is a set of mass and dimensional parameters of the rover, and third is a set of soil parameters.

### Wheel/Soil Interaction Model

The fundamental equation for wheel/soil interaction is Coulomb's equation:

$$\tau_m = c + \sigma_m \tan \phi$$

where  $\tau_m$  and  $\sigma_m$  are the maximum shear stress and normal stress at the wheel/soil interface,  $c$  is the coefficient of soil cohesion and  $\phi$  is the internal friction angle (of the soil).

Coulomb's equation can be modified to account for other aspects of the wheel/soil interface geometry. Following Iagnemma [10], the shear stress can be written as

$$\tau_m = (c + \sigma_m \tan \phi) \left( 1 - e^{-\frac{r\theta}{2k}} \right)$$

where  $r$  is the radius of the wheel,  $\theta$  is the angle of the contact region, and  $k$  is a constant. This equation follows from equations (19) and (20) in Iagnemma by setting  $i = 1$ .

Multiplying Coulomb's equation by the area of contact gives an estimate of the traction force  $H$  in terms of the wheel/soil interaction geometry, soil parameters, and weight  $W$  acting on the wheel.

$$H = (Ac + W \tan \phi) \left( 1 - e^{-\frac{r\theta}{2k}} \right)$$

The contact area for each wheel can be expressed as

$$A = br\theta$$

where  $b$  is the width of the wheel.

### Rover Parameters

The Rocky 8 rover with a 5 DOF arm and Mast weighs 62 kg. The wheel diameter is 0.200 m and the wheel width is 0.123 m.

### Soil Parameters

Soil parameters for a small range of Earth terrain can be found in Table 1 of Iagnemma. For Sandy Loam, the maximum rover traction is estimated to be 262 N (59 lb). This agrees surprisingly well with some rough force measurements of dragging the Rocky 8 rover over sand (average of about 55 lb).

Soil parameters for Mars are estimated from measurements taken from the Viking, Pathfinder, and MER missions. Representative corresponding values for  $c$  and  $\phi$  are as follows (we assume a value of  $k = 0.025$ ):

$$c = 1.7 \text{ kPa and } \phi = 20^\circ \text{ (VK1)}$$

$$c = 1.1 \text{ kPa and } \phi = 35^\circ \text{ (VK2)}$$

$$c = 0.25 \text{ kPa and } \phi = 35^\circ \text{ (PF)}$$

$$c = 5 \text{ kPa and } \phi = 20^\circ \text{ (MER)}$$

The only other change to estimate traction forces on Mars is to use Mars gravity

$$g = 3.693 \frac{m}{s^2}$$

## 6. CORING TESTBED

A testbed was developed for testing coring from a manipulator, as shown in Figure 0. A four DOF arm was equipped with a 6-axis force-torque sensor and a commercial coring tool. A compliant mount was used between the tool and force-torque sensor to minimize vibration from the tool to the arm. Cores that were acquired were generally broken up which indicated that quality of core is an important issue. Alternative coring tools and mounting approaches are being considered.

## 7. RESULTS

Prediction of wheel-soil slippage is difficult due to the wide variety of soil types and wheel configurations relative to the soil. MER mission operators purposely wiggle the wheels before performing a Rock Abrasion Tool (RAT) operation. The RAT tool on the arm turret requires a preload against a rock surface and the wheels are wiggled in order to sink the wheels into the soil to provide a more stable platform for the RAT operation. To get an idea of the scope of the problem for coring from a low-mass rover, parameters of the Rocky8 research rover were put into the wheel-soil interaction model [10] to determine whether that rover would slip in expected Mars sampling conditions. The rover is of a similar scale as expected for a small sampling

rover. It has a six-wheel rocker-bogie configuration and weighs 62 kg, (see Figure 0). The traction of the rover on horizontal and 25 degree slopes were computed using the wheel-soil interaction models. The results are shown in Table 0.

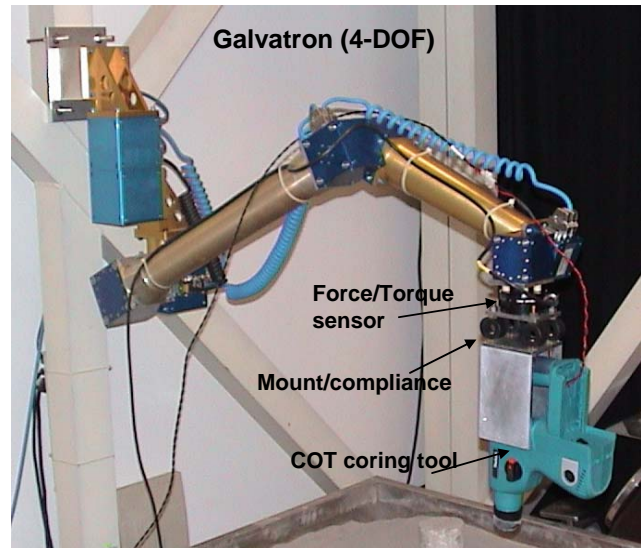


Figure 11. Coring testbed

Cores acquired using the commercial rotary percussive coring tool were of low quality, generally broken in many pieces. We have therefore procured a new commercial coring tool that has less impact energy. Also, we are planning on testing other coring tools. Work in the next year will include determination of the need for bracing a coring tool against the environment to provide needed tool stability and determining what type of coring tool to use for the coring operation from a low-mass rover. Also coordinated rover-arm control approaches to enable continued coring after rover slippage will be investigated.





**Figure 12. Rocky8 rover in JPL marsyard**

**Table 2. Predicted traction on Mars terrains**

Location	Horizontal Traction (N)	25° Slope Traction (N)
Viking 1	97	Negative, slips
Viking 2	132	25
Pathfinder	110	4
MER	117	15

## 8. CONCLUSIONS

Coring from a low-mass rover provides new technical challenges where the rover cannot be assumed to be a stationary platform during the coring operation. Coring tool models have been developed to help in the selection of the best type of coring tool to use when coring from a low-mass rover. A simulation environment has been developed to simulate coring from a low-mass rover. A testbed has been developed to test coring from a manipulator. Current results show that stability of the coring tool relative to the environment during the coring operations is important in obtaining an intact core sample. On-going work will focus on providing a stable tool relative to the environment.

## ACKNOWLEDGEMENTS

The research described in this paper was carried out at the Jet Propulsion Laboratory, California Institute of Technology, under a contract with the National Aeronautics and Space Administration as part of the Mars Technology Program.

## REFERENCES

- [1]. A. F. C. Haldemann, E. T. Baumgartner, G. H. Bearman, D. L. Blaney, D. I. Brown, B. P. Dolgin, L. I. Dorsky, T. L. Huntsberger, A. Ksendzov, J. C. Mahoney, M. J. McKelvey, B. E. Pavri, G. A. Post, E. F. Tubbs, R. E. Arvidson, N. O. Snider, S. W. Squyres, S. Gorevan, G. Klingelhofer, B. Bernhardt, and R. Gellert, "FIDO science payload simulating the Athena Payload," *Journal of Geophysical Research*, Vol. 107, No. E11, 8006, doi: 10.1029/2001JE001738, 2002
- [2]. M. Bruno, G. Han, and C. Honeger, "Advanced Simulation Technology for Combined Percussion and Rotary Drilling and Cuttings Transport," *GasTIPS*, Winter, 2005.
- [3]. T. Myrick, , S. Gorevan, C. Batching, S. Stoescu, M. Maksymuk, K. R. Davis, M. A. Umyy, and the Athena Science Team, "The Athena miniature rock coring and rock core acquisition and transfer system (Mini-Corer)," in *Workshop on Concepts and Approaches for Mars Exploration*, abstract 6105, Lunar and Planet. Inst., Houston, Tex., 2000.
- [4]. X. Bao, Y. Bar-Cohen, Z. Chang, B. P. Dolgin, S. Sherrit, D. S. Pal, S. Du, and T. Peterson, "Modeling and Computer Simulation of Ultrasonic/Sonic Driller/Corer (USDC)" *IEEE Transaction on Ultrasonics, Ferroelectrics, and Frequency Control (UFFC)*, Vol. 50(9), p. p. 1147-1160, 2003.
- [5]. A. Batako, V. Babitsky, and N. Halliwell, "A Self-Excited System for Percussive-Rotary Drilling", *Journal of Sound and Vibration*, Vol. 259(1), p.p. 97-118, 2003.
- [6]. K.-S. Chang and O. Khatib, "Operation Space Dynamics: Efficient Algorithms for Modeling and Control of Branching Mechanisms", *Proceedings of the International Conference on Robotics and Automation*, 850--856, 2000
- [7]. O. Khatib, "A Unified Approach to Motion and Force Control of Robot Manipulators: The Operational Space Formulation", *Int. J. Robot. Automa.*, **3**(1), 43--53, 1987.

- [8]. O. Khatib, O. Brock, K. Chang, F. Conti, D. Ruspini, and L. Sentis, "Robotics and Interactive Simulation", *Communications of the ACM*, **45**(3), 46--51, March 2002.
- [9]. D. Ruspini and O. Khatib, "Collision / Contact Models for Dynamic Simulations and Haptic Interaction", *Proceedings of the International Symposium on Robotics Research*, 185--195, 1999.
- [10]. K. Iagnemma, S. Kang, H. Shibly, and S. Dubowsky, "Online terrain parameter estimation for wheeled mobile robots with application to planetary rovers," *IEEE Transactions on Robotics*, 20(5): 921-927, October 2004.

## BIOGRAPHY



**Paul Backes, Ph.D.** is the Group Supervisor of the Mobility and Manipulation group at Jet Propulsion Laboratory, California Institute of Technology, where he has been since 1987. He received the BSME degree from U.C. Berkeley in 1982 and Ph.D. in 1987 in Mechanical Engineering from Purdue University.

Dr. Backes received the 1993 NASA Exceptional Engineering Achievement Medal for his contributions to space telerobotics, 1998 JPL Award for Excellence, 1998 NASA Software of the Year Award Sole Runner-up, and 2004 NASA Software of the Year Award. He has served as an Associate Editor of the *IEEE Robotics and Automation Society Magazine*.



**Oussama Khatib, Ph.D.** is a Professor of Computer Science at Stanford University. He received his Ph.D. in 1980 from Sup'Aero, Toulouse, France. His current research is in human-centered robotics, human motion synthesis, humanoid robotics, dynamic simulation, haptic interfaces, and human-friendly robot design.

This builds upon a large body of work pursued over the past 25 years and published in over 200 contributions in the field. Professor Khatib was Program Chair of ICRA2000 and editor of *The Robotics Review*. He served as director of the Stanford Computer Forum and is currently president of the International Foundation of Robotics Research and editor of *Springer Tracts in Advanced Robotics*. Professor Khatib is an IEEE Fellow, a Distinguished Lecturer of IEEE, and a recipient of the JARA Award.



**Dr. Antonio Diaz-Calderon** Antonio Diaz-Calderon is a member of Information Systems and Computer

Science Staff with the Mobility and Manipulation Group at the Jet Propulsion Laboratory, Pasadena, CA. His research work at JPL involves manipulation kinematics, optimal estimation and motion control. He received the BSEE in 1987 and the M.S. in Computer Science in 1990 from Monterrey Institute of Technology (Mexico City, Mexico), and M.S. in 1993 in Engineering and Ph.D. in 2000 in Electrical and Computer Engineering from Carnegie Mellon University. He held a Post-Doctoral Fellowship appointment with The Robotics Institute at Carnegie Mellon University (2000-2001), and a faculty appointment as Commercialization Specialist with The Robotics Institute (2001-2003). While at the Robotics Institute Dr. Diaz-Calderon developed an estimation-based tipover sensing system to enhance dynamic stability of heavy articulated machines, robust position estimation algorithms for the PerceptOR program and vehicle dynamic models used for mobility analyses on prototype vehicles for Future Combat Systems' Unmanned Ground Combat Systems (UGCV), and Gladiator. His research interests include: sensor fusion and state estimation, and rover navigation and mobility.



**James Warren** is a Ph.D. candidate in the Artificial Intelligence Laboratory at Stanford university. He received his B.S. degree in Mathematics from Texas A&M University in 1996 and his M.S. degree in Scientific Computing and Computational Mathematics in 2000. His research is in identifying human motion behaviors

from motion capture data and applying these strategies for humanoid robotic control.



**Curtis Collins, Ph.D.** received the B.S. Degree in Bioengineering, from the University of California, San Diego, and the M.S. and Ph.D. Degrees in Mechanical Engineering from the University of California, Irvine. After completing his degree he taught kinematic, robotics, and design at the California Institute of

*Technology, the University of California, Riverside, and the University of California, Irvine. While at Caltech, he helped to restructure the Mechanical Engineering Design Laboratory course and continues to work with faculty to improve student design experience. Dr. Collins joined JPL in 2005. His research interests include the design and analysis of parallel and multi-limbed mechanisms, simulation and visualization of multi-loop mechanical systems, and novel kinematic and mechanical designs for advanced mobility systems.*



**Zensheu Chang, Ph.D.** is an engineer at Jet Propulsion Laboratory, California Institute of Technology. Dr. Chang received his MS degree from National Taiwan University in 1988, and Ph.D. degree in Mechanical and Aerospace Engineering from University of California, Los Angeles in 1997. His research areas include structural dynamics, ultrasonic NDE/NDT, piezoelectric actuators, CAD/FEM modeling, elastic wave propagation, and solid mechanics. He has published more than 50 papers in related research areas.

